ADVANCED SUSTAINABLE SYSTEMS
www.advsustainsys.com

An Innovative Sunlight-Driven Device for Photocatalytic Drugs Degradation: from laboratory- to real-Scale Application. A First Step Toward Vulnerable Communities

Melissa Greta Galloni, Ermelinda Falletta, Milad Mahdi, Giuseppina Cerrato, Alessia Giordana, Daria Camilla Boffito, and Claudia Letizia Bianchi*

Freshwater represents one of the most precious resources on the planet, so it is fundamental to preserve it. In this work, an innovative sunlight-driven device composed of bismuth oxybromide (BiOBr) grown on a material derived from natural sources, i.e., Lightweight Expanded Clay Aggregates (LECA), is developed to clean surface waters under natural solar light irradiation. For this purpose, the photodegradation of two non-steroidal anti-inflammatory drugs, ibuprofen, and diclofenac, is investigated under varying operative conditions. Laboratory- and real-scale experiments reveal that the fabricated floating BiOBr/LECA photocatalyst fully degrades diclofenac, whereas limited abatement of ibuprofen is observed. Based on the identification of specific transformation products (TPs) during the degradation, this behavior seems to be strongly related to the different structures of the two drugs. In fact, the main TP produced during diclofenac degradation derives from dechlorination and ring condensation: this type of photocatalytic degradation pathway is generally favored over the C—C bonds's cleavage, which is a unique possibility for IBU abatement. Moreover, the potential partial adsorption of these species on the photocatalyst's active sites can cause their deactivation. Finally, reusability tests demonstrate the high stability of the floating composite.

1. Introduction

Nowadays, contamination of fresh water is a global concern. Water use has been growing globally in the last century at more than twice the population rate increase. Population growth puts unprecedented pressure on water resources, especially in arid regions. Food and Agriculture Organization of the United Nations (FAO) estimated that 1800 million people are expected to live in countries affected by water scarcity by 2025.[1] This issue is ever more pronounced in developing countries, where water scarcity is also responsible for numerous pandemic crises, during which unsanitary conditions put patients and doctors at risk for disease transmission.[2] World Health Organization (WHO) revealed that a significant part of these infections is ascribed to the lack of clean water and the consequent inefficient hygiene protocols. Urban areas also contribute to water scarcity, since organic solvents, contaminants, and heavy metals from disposal sites and storage facilities are continuously released into water sources. Further, the agriculture sector is responsible for the uncontrolled release of pesticides and fertilizers, and human and animal wastes are the main factors in discharging harmful microorganisms into surface waters.[3]

Ibuprofen (IBU) and diclofenac (DCF) are the two most known non-steroidal anti-inflammatory drugs (NSAIDs) widely used in medicine,[4] whose market size stood at USD 15.58 billion in 2019 and is projected to reach USD 24.35 billion by 2027.[5] IBU is the methyl-4-[isobutyl] phenylacetic acid used for the treatment of fever, muscle pain, arthritis, migraine, and toothaches,[6–8] strongly impacting the environment, even

M. G. Galloni, E. Falletta, M. Mahdi, C. L. Bianchi
Dipartimento di Chimica
Università degli Studi di Milano
via Camillo Golgi 19, Milano 20133, Italy
E-mail: ermelinda.falletta@unimi.it

The ORCID identification number(s) for the author(s) of this article can be found under https://doi.org/10.1002/adsu.202300565

DOI: 10.1002/adsu.202300565

M. G. Galloni, E. Falletta, G. Cerrato, A. Giordana, C. L. Bianchi
Consorzio Interuniversitario Nazionale per la Scienza e Tecnologia dei Materiali (INSTM)
Via Giusti 9, Firenze 50121, Italy

G. Cerrato, A. Giordana
Dipartimento di Chimica
Università degli Studi di Torino
via Pietro Giuria 7, Torino 10121, Italy

D. C. Boffito
Polytechnique Montréal
Génie Chimique 2900 Boul, Edouard Montpetit, Montréal, QC H3T 1J4, Canada

in small concentrations.[9,10] DCF belongs to the phenylacetic acid class with anti-inflammatory, analgesic, and antipyretic features. It usually treats pain and helps alleviate arthritis symptoms (e.g., stiffness, swelling, and joint pain).[11–13] In the last decades, their consumption has drastically increased due to the rapid growth and aging of the world population, thus contributing to the increase of their concentration in surface waters,[10,13,14] consequently destroying the aquatic ecosystems and organisms.[15]

In the above-depicted panorama, the possible purification and reuse of wastewater still represents an unavoidable challenge, since the demand for freshwater due to population growth, drought, and intensive consumption in the agricultural/industrial sectors is continuously increasing.[16] In this context, researchers are working on the development of novel, efficient strategies aimed at the abatement of NSAIDs from the environment: among them, advanced oxidation processes (AOPs) have emerged.[17–20] Thanks to the use of a semiconductor and solar light, oxidants, like hydroxyl (HO·), peroxyl (O_2^{-}·), and hydroperoxide (HO_2·) radicals can be produced to mineralize organic contaminants to carbon dioxide and water.[21] Following this path, solar light irradiates the photocatalyst surface, which can absorb an equal or higher amount of energy than its bandgap. In this way, an electron is prompted to move from the valence band (VB) to the conduction band (CB), generating an electron-hole pair, producing and promoting redox reactions.[22,23] This process could be exploitable in countries where solar irradiation is abundant throughout the year.

Photodegradation of IBU and DCF have been investigated in several works, in which nano- and micro-powder photocatalysts, ranging from conventional formulations based on titania[24] and zinc oxide[25,26] to more sophisticated ones (e.g., heterojunctions, etc.), have been proposed.[13,27,28] In this framework the use of materials in powder form remains limited from a practical viewpoint due to the difficult separation and/or recovery from the reaction mixture for sustainable reuse.[20,29,30] In particular, the powder use could invalidate the selected strategy due to its incomplete recovery, causing contamination issues. In fact, if, on the one hand, working on fine powders has several benefits (e.g., high dispersion, impressive photoactivity, etc.), on the other , scale-up issues need to be addressed. Therefore, immobilization strikes a compromise between the benefits of the photocatalysts and the necessity to ensure their appropriate application by improving stability and facilitating simpler handling. Since 1993 researchers have been developing floating photocatalysts as sustainable and efficient alternatives.[31,32] Floating photocatalysts maximize both light utilization and surface aeration, since they float on the air-water interface. At the same time, their use also decreases the post-treatment cost.[33,34] Over the years, different supports (e.g., perlite, vermiculite, glass, cork, graphite, polymer, and alginates) have been selected for anchoring the photocatalytic active phase on them, producing floating photocatalysts to degrade pollutants present in wastewaters. However, to date, there is still no simple, economical, and accessible method, allowing the application of photocatalysis for water purification in communities with limited access to clean water.

In fact, each studied system has revealed some limitations, like poor stability, difficulties in stably anchoring the photocatalytic active phase, and low stability, which are objects of the current research studies.[34–37] In this context, considering the high potential of the application of these systems, when developed correctly in a way to be sustainable and efficient, hard research efforts have to be placed in this frame to propose eco-friendly alternatives to conventional systems in powder form.[35,38–40]

Light-expanded clay aggregates (LECA) are cheap man-made manufactured from natural materials traditionally used in construction industries. LECA is extremely light, chemically inert, and thermally stable up to 1000 °C, and it is characterized by low density and high porosity, conferring the ability to be floatable on water.[41,42] All these peculiarities make it a suitable candidate to be exploited as a support in floating photocatalysts. To the best of our knowledge, just a few works have reported the use of properly modified LECA as adsorbent for wastewater treatment.[43–45] Other researchers have tried to develop hybrid photocatalysts based on LECA for aqueous ammonia or dye degradation. More in detail, Hosseini et al. anchored titanium dioxide (TiO_2) nanoparticles onto LECA for the first time, giving rise to an interesting floating photocatalyst for almost complete ammonia degradation within 300 min.[46] However, this material required further optimization due to its wide band gap (3.0–3.2 eV), causing poor visible light utilization, high recombination of the photogenerated electron-hole pairs, and unstable anchoring at the LECA surface.[46] Kakehazar and coworkers fabricated a floating TiO_2/LECA composite for the degradation of ammonia in the petrochemical waste. In addition, they designed and optimized a proper solar photocatalytic reactor that efficiently removes the ammonia content in the waste at basic pH, proposing an alternative to the existing ones.[47] Subsequently, Shavisi et al. proposed a hybrid structure composed of TiO_2-ZnO/LECA to fully abate 400 mg·L^{-1} aqueous ammonia at basic pH in the presence of 25 g·L^{-1} catalyst dosage within 3 h UV irradiation.[48] Eventually, the group of Rahimpour moved toward applying a modified LECA-based material composed of ZnO to remove reactive yellow 84, achieving the complete abatement of the dye (50 mg·L^{-1}) at acidic pH under UV irradiation.[49]

However, most of these examples refer to the use of TiO_2 as a photocatalytic active phase, although many criticisms are related to it, as recently reported by Pulgarin et al.[24]

Recently, bismuth oxybromide (BiOBr) has been recognized to possess unique physico-chemical features, deserving to be exploited to produce a promising photocatalytic active phase exploitable in several fields, ranging from hydrogen evolution to nitrogen reduction and wastewater remediation.[50–52] In this scenario, numerous researchers largely studied the potentialities of using BiOBr in powder for environmental remediation issues. Among them, in a recent work Falletta et al. demonstrated that BiOBr in powder form can efficiently photodegrade ibuprofen from water thanks to its bandgap value, morphology, and piezoelectric behavior.[53]

Following these premises, herein we propose for the first time the preparation, characterization, and optimization of a novel sustainable floating photocatalytic system composed of BiOBr grown on LECA (BiOBr/LECA) to efficiently photodegrade two model drugs, i.e., ibuprofen and diclofenac, usually present in real surface waters, to alleviate water contamination in critical contexts, such as those of vulnerable communities.

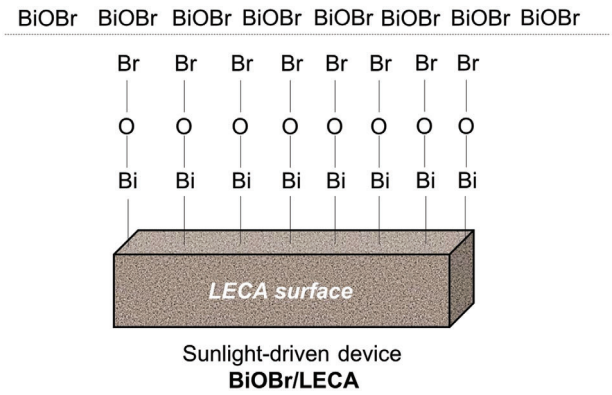

Scheme 1. BiOBr growth on LECA.

2. Results and Discussion

2.1. BiOBr/LECA characterization

Floating photocatalysts represent a new generation of materials to be applied in real conditions since they permit the maximization of the surface aeration of the active phase and, at the same time, its irradiation. Moreover, the possibility of using an immobilized photocatalyst overcomes the limits given by employing dispersed powders, guaranteeing the easy recovery of the material.

In this context, as a preliminary point, the porosity of pristine LECA was evaluated by BJH model from the desorption branch of N_2 adsorption/desorption isotherms at −196 °C. Figure S1 (Supporting Information) reports the obtained results, confirming the intrinsic mesoporosity of the pristine LECA, according to the literature.[42,43]

Three floating photocatalysts composed of BiOBrX/LECA with different percentages of active phase (X = 3, 6, and 11 wt.%) were then prepared via wet impregnation, directly synthesizing BiOBr onto LECA (**Scheme 1**).

The surface of pristine LECA is rich in SiO_2, Al_2O_3, Fe_2O_3, CaO, and other alkalis, such as Na_2O and K_2O, according to the literature[41] and the EDS investigation. Putting in contact the pristine LECA with Bi^{3+} precursor, this latter can be easily anchored on the surface of the clay, or can partially replace the main natural cations (mainly Na^+ and K^+). These Bi^{3+} centers act as nuclei for the BiOBr growth after KBr addition.

Pristine LECA and BiOBr11/LECA, the most promising material in terms of photodegradation efficiency, were characterized by selected characterization techniques, whose results are described below.

Field Emission Scanning Electron Microscopy (FESEM) and Energy-Dispersive X-ray Spectroscopy (EDS) investigated the samples' morphology and materials composition (**Figures 1** and S2, Supporting Information). Pristine LECA and BiOBr11/LECA samples exhibit slightly different external and internal morphology. In the case of plain LECA (sections a and b in Figure 1), the presence of pores is clear with a wide array of sizes, and external and internal surfaces appear as rough. When BiOBr is added, the morphology tends to be more roundish, still being porous (sections c and d in Figure 1). Moreover, at higher magnification the clear presence of small particles is evident. These particles exhibit the typical features of BiOBr based on the shape and literature data as well (Figure S2d, Supporting Information).[53]

In Figure S2c (Supporting Information) a relevant FESEM image of the BiOBr11/LECA composite is reported and leads to the identification of BiOBr aggregates with the typical flower-like morphology, in which individual lamellae are evident (the average thickness of the lamellae falls in the 40–70 nm range).[53]

In Figure S2 (Supporting Information) the relevant EDS analyses of both materials are reported, thus confirming the presence of Bi and Br species when added.

Sample phase composition was further investigated by X-ray powder diffraction (XRPD). **Figure 2** shows the collected diffractograms of LECA and BiOBr11/LECA compared with the standard JCPDS file of the tetragonal BiOBr phase (JCPDS 01−078−0348). As the first step, the XRPD pattern of the pristine LECA confirmed its mineralogic composition, according to FESEM images. In particular, the pronounced X background indicated the presence of the amorphous phase typical of the natural LECA sample.[43–45] Moreover, the LECA diffractogram revealed the characteristic peaks of quartz, anorthite, calcite, and dolomite, according to Kalhori et al.[45] The diffractogram of BiOBr11/LECA showed the main diffraction peaks at ≈10.8, 21.8, 25.2, 31.7, 32.2, 39.3, 46.3, 50.7, 53.4, 57.2° indexed to the corresponding (001), (002), (101), (102), (110), (112), (200), (104), (211), (212) planes of the tetragonal BiOBr phase (JCPDS 01−078−0348) as well as additional peaks at 26.6, 36.5, 42.4, 44.8, 50.1, 65.4, 68.1°, ascribed to LECA.[43,53] These data confirmed the copresence of BiOBr and LECA in the prepared floating photocatalyst, demonstrating that BiOBr was successfully synthesized onto LECA.

Determining the point of zero charge (pH_{pzc}) is a fundamental step to elucidate the photocatalyst behavior.[54] In the case of composite materials, the pH_{pzc} evaluation is critical because, if the first component is not homogeneously distributed on the second one, the two charged surfaces can compete or operate oppositely for pollutant adsorption. In particular, the pH_{pzc} depends on different factors (e.g., chemical/physical structure of the studied sample surface, pH medium, *etc.*),[54] and provides information about the type of charges, which depend on the acidic and/or basic sites, prevailing at the material surface. More specifically, when the pH is below the pH_{pzc}, the material surface is positively charged; thus, anions are attracted to it. Differently, when the pH is above the pH_{pzc}, it is negatively charged, thus attracting cations. However, numerous results are reported in the literature,[55] no unique pH_{pzc} value is reported for each single chemical compound because the pH_{pzc} parameter relies on the specific surface properties (e.g., defects or OH groups present on the oxides surface, number/type of functionalization, etc.), which can also change depending on the synthetic approaches used. According to these premises, the pH_{pzc} of both pristine LECA and BiOBr11/LECA was measured and corresponded to 5.65 and 7.75, respectively (**Figure 3**). If the pH_{pzc} of pristine LECA matches with other results previously reported in the literature,[44] on the other hand, that of BiOBr11/LECA was similar to the value reported in the literature for BiOBr powder,[53] confirming that the coating of LECA with the photocatalyst occurred successfully.

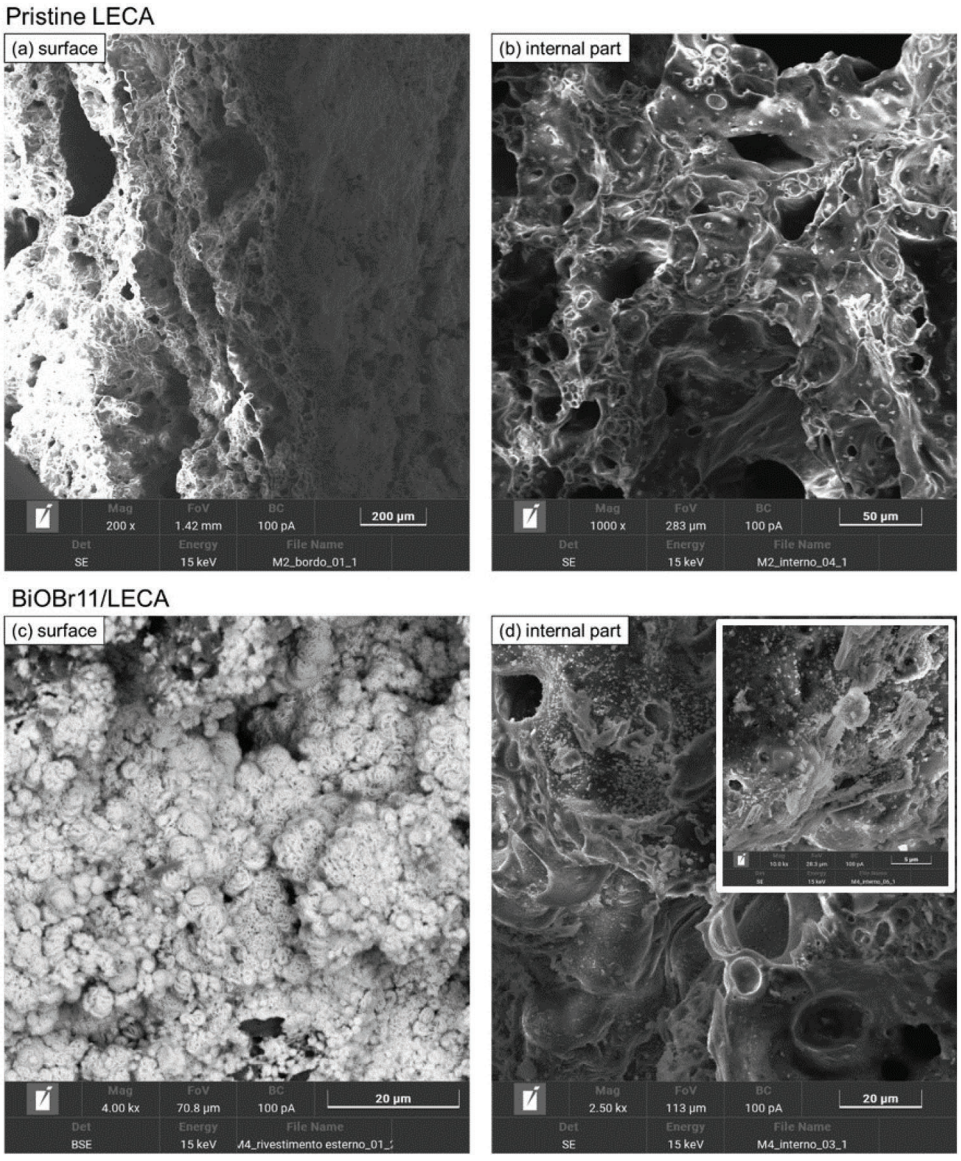

Figure 1. FESEM images of pristine LECA and BiOBr11/LECA at different magnifications.

In the conditions selected for the photodegradation tests (neutral pH for ultrapure water, UW, and slightly alkaline pH for simulated drinking water, DW), both IBU and DCF are negatively charged (pKa of 4.85 and 4.15, respectively).[56] However, although in both cases, the pollutants' adsorption onto the catalyst surface should be unfavoured, the exposed positive charges of BiOBr on LECA in the BiOBr11/LECA composite were sufficient to guarantee pollutants adsorption and its subsequent abatement, as demonstrated by the degradation tests.

2.2. Ibuprofen and Diclofenac Abatement Tests

The photocatalytic activity of the fabricated BiOBrX/LECA samples was evaluated in the degradation of IBU and DCF under solar light irradiation. In particular, two different tests were performed: laboratory- and real-scale tests in ultrapure or simulated drinking water (UW and DW), respectively. The obtained results are discussed below.

2.3. Laboratory-Scale Tests

The photocatalytic activity of the floating BiOBrX/LECA composites was evaluated toward the abatement of IBU and DCF in both UW and DW by laboratory-scale tests in the presence of magnetic stirring.

At first, the photodegradation activity of the floating composites was investigated toward IBU abatement in UW (**Figure 4**). The catalyst dosage was set to 3 g to guarantee proper aeration of the water mixture and, at the same time, effective light penetration.

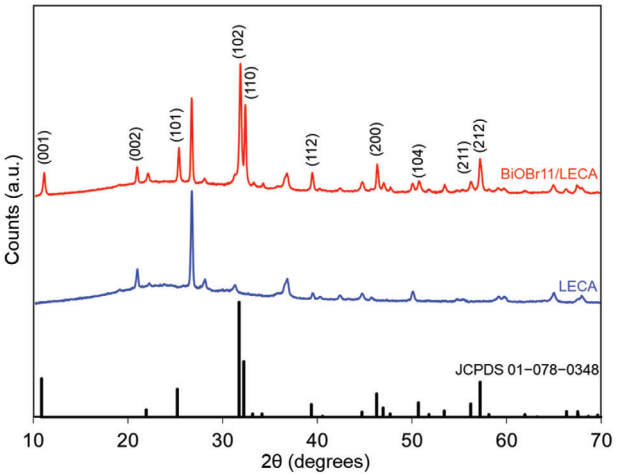

Figure 2. XRPD patterns of LECA and BiOBr11/LECA compared to the reference diffraction pattern of BiOBr (JCPDS 01–078–0348).

According to the point of zero charge, the adsorption capacity of the floating composites, as well as of bare LECA (Figure 4), was low (below 10%), independently of the BiOBr content, thus ensuring that this step did not impact on the photodegradation. An additional 3 h adsorption experiment under dark was carried out in the presence of the composite with the highest BiOBr content (BiOBr11/LECA), which confirmed this result (Figure S3, Supporting Information). As shown in Figure 4, the photocatalytic activity of BiOBrX/LECA under solar light irradiation is strongly related to the BiOBr loading. In fact, by increasing the BiOBr content on LECA (from 3 to 11 wt.%), the IBU degradation rate speeds up significantly. In particular, BiOBr3/LECA achieved 87% IBU removal within 240 min, whereas both BiOBr6/LECA and BiOBr11/LECA could completely remove the drug within 120 min and 210 min solar irradiation, respectively. Therefore, since 11 wt.% BiOBr was the most beneficial dose, the BiOBr11/LECA composite was selected for the successive investigations.

The transformation products (TPs) of the IBU degradation by BiOBr11/LECA were identified by UPLC/MS analyses. Figure S4 (Supporting Information) shows the time-resolved profiles of the identified TPs obtained during the IBU photodegradation that are in accordance with the literature.[53]

The effect of the water matrix in the IBU degradation was investigated (**Figure 5**), elucidating that when the process is carried out in DW, the floating photocatalyst becomes less efficient, reaching ≈80% IBU abatement in 240 min, suggesting a competitive effect of the ions in solution.

Similar results were obtained in a previous work where BiOBr was used in the form of dispersed powder,[53] confirming that the immobilization of the photocatalyst on the floating support does not compromise its activity.

To extend the application of the floating composite to other pollutants, the photocatalytic behavior of the studied material was investigated toward DCF abatement. The obtained results are reported in Figure 5b. As previously observed for IBU removal, a low adsorption behavior was also detected in this case in the first 30 min in both UW and DW in dark conditions. However, unlike what was observed during the IBU degradation, under light irradiation BiOBr11/LECA exhibited an extraordinary photodegradation activity toward DCF, achieving the complete degradation of the pollutant after 90 min and 210 min in UW and DW, respectively. The water matrix seems not to influence the photocatalytic activity of the material. However, regarding the DCF photodegradation test, a main transformation product (TP) with a retention time of 6.7 min was detected (Figure S5, Supporting Information). UPLC/MS analyses were carried out to identify it. According to Meroni et al.,[14] TP259 was identified in agreement with the dechlorination pathway. In addition, additional unknown TPs were identified by HPLC, but MS did not detect them.

To gradually move toward real applications, BiOBr11/LECA was applied for the photodegradation of a mixture of the two drugs (25 mg·L^{-1} IBU and 25 mg·L^{-1} DCF in UW) and the results are displayed in **Figure 6a**. Surprisingly, BiOBr11/LECA achieved complete DCF degradation within 90 min, resulting in ineffective IBU removal.

Although empirical evidence of this result has not yet been found, it is possible to hypothesize that the adsorption of DCF TPs on the catalyst's surface inhibits the activity of the active sites toward IBU degradation.

However, as shown in Figure 6, reducing the global drug concentration, the photodegradation of DCF was still complete, whereas IBU experienced a partial abatement that became complete, reducing the total concentration of drugs up to 10 mg·L^{-1}. This confirms that the availability of free active sites is crucial to remove both pollutants.

Further investigations were conducted to clarify the role of DCF and its TPs in deactivating the photocatalyst. The activity of BiOBr11/LECA were explored in the photodegradation of a mixture of IBU and DCF at different concentrations in solution, but maintaining the total drugs concentration to 50 mg·L^{-1}. **Figure 7** shows the results obtained for the DCF/IBU weight ratio corresponding to 6:1, 3:1, 1:3, and 1:6, respectively. DCF was fully degraded in all tests regardless of the DCF/IBU ratio. In contrast, the photodegradation capacity of the floating composite toward IBU abatement is strongly affected by the solution composition. In particular, the IBU removal increases, decreasing the starting DCF concentration in the solution. In fact, from the DCF/IBU ratio of 6:1 to 1:6 the percentage of IBU abatement increases from ≈ 35 to 85%. The photocatalytic activity of BiOBr11/LECA toward IBU degradation seems to be correlated to the formation of TP259, which could be adsorbed on the active sites, causing their deactivation.

The above-described experiments clearly demonstrated the potential as well as the limitations of this type of floating catalyst as a sunlight-driven photocatalytic system for pollutant degradation in water. The next step regarded verifying the floating photocatalyst, BiOBr11/LECA, performances in real-scale tests.

2.4. Real-scale tests

Two different bowls were employed for the real-scale tests: one made of transparent glass and the other of white polypropylene to verify the effect of light penetration in the photocatalytic process. All tests were conducted by exposing the setup under natural solar light irradiation for three days, according to the details reported in the Experimental Section. Data related to the

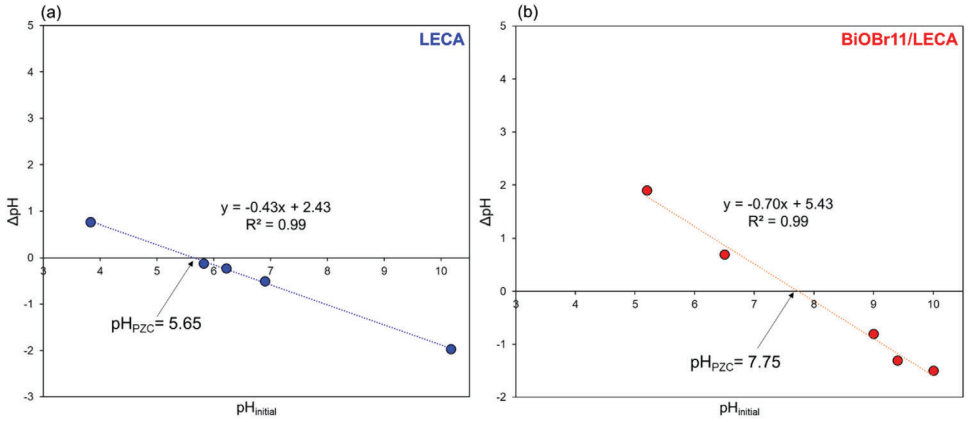

Figure 3. Point of zero charge of pristine a) LECA and b) BiOBr11/LECA.

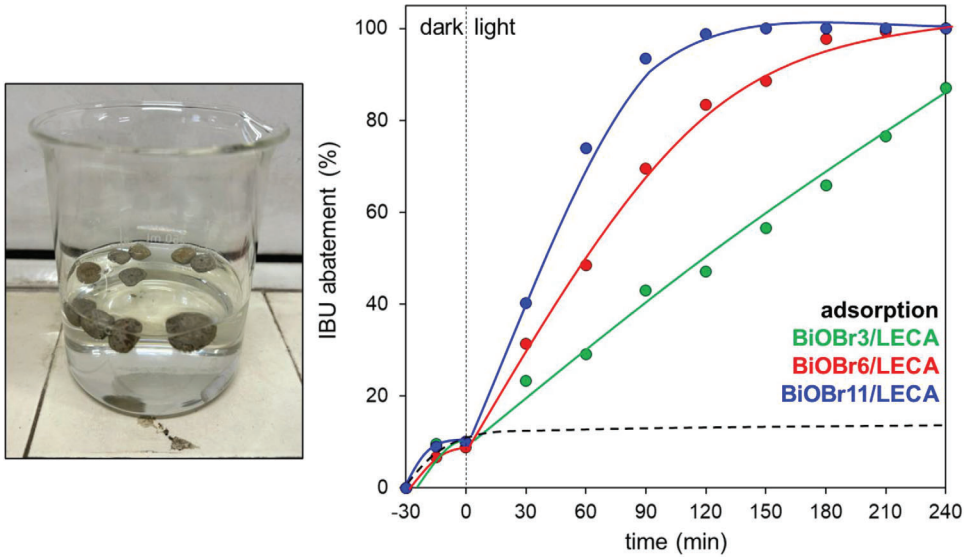

Figure 4. Effect of BiOBr loading onto LECA toward IBU photodegradation in UW. Experimental conditions: IBU concentration = 50 mg·L^{-1}; catalyst dosage = 3 g BiOBrX/LECA; solar light irradiation = 35 W·m^{-2}.

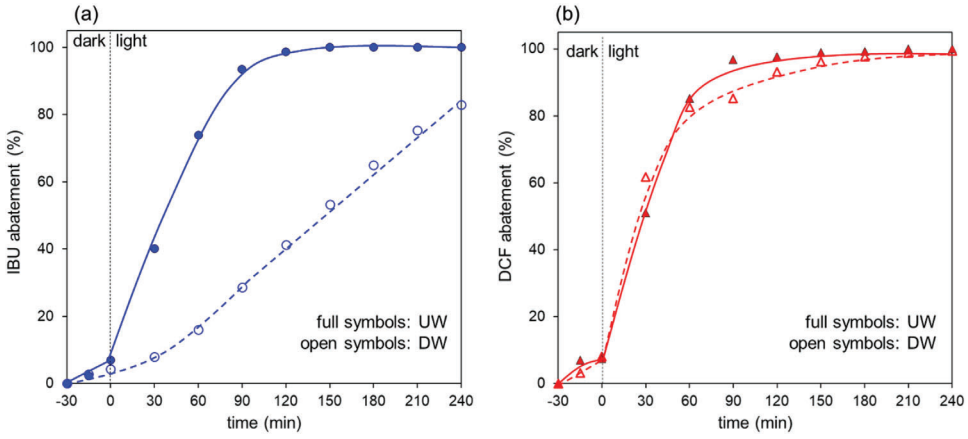

Figure 5. Drugs photodegradation by 3 g BiOBr11/LECA: effect of water matrix (UW and DW) on IBU or DCF degradation (a and b panels, respectively). Experimental conditions: single drug concentration = 50 mg·L^{-1}; solar light irradiation = 35 W·m^{-2}.

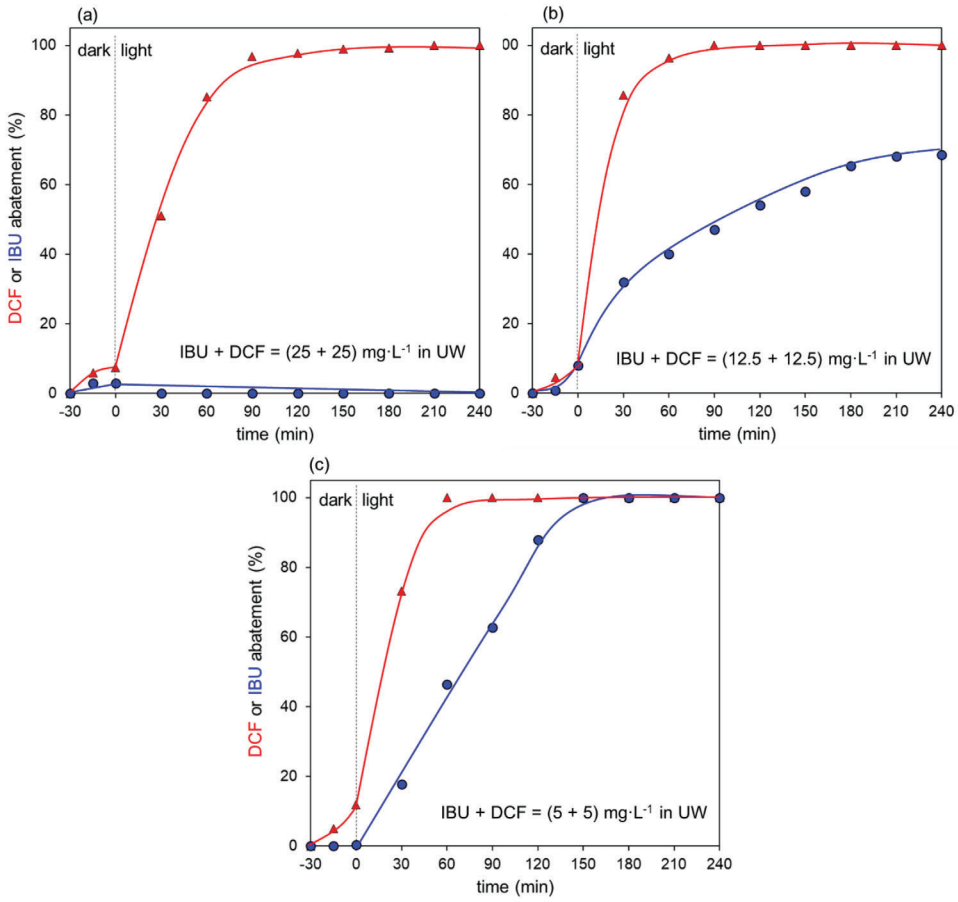

Figure 6. Photodegradation results of drugs mixture (1:1 weight ratio) by 3 g BiOBr11/LECA. Total drug concentration (IBU + DCF) = 50, 25, and 10 $mg \cdot L^{-1}$. Solar light irradiation = 35 $W \cdot m^{-2}$.

daily medium solar irradiation of the place in which all tests were performed (campus Città Studi of Università degli Studi di Milano, Italy, where the Dipartimento di Chimica is located) were retrieved from the Arpa Lombardia database.[57]

In this case, the tests were carried out without magnetic stirring in DW to simulate a real scenario. A preliminary test carried out using the lab-scale setup demonstrated a lower photocatalytic degradation of IBU in the absence of stirring, achieving only ≈ 60% IBU abatement within 240 min (Figure S6, Supporting Information). However, this demonstrates that, despite the absence of any external force that allows its rotation (wind, manual stirring, etc.), the spherical shape of the composite allows an effective refresh of the catalyst.

Figure 8 displays the results obtained for the tests carried out in the two different bowls on a real scale. In both cases, the floating photocatalyst (BiOBr11/LECA) was able to completely degrade DCF, whereas the IBU abatement was lower, reaching ≈ 80%, confirming the result obtained in the lab-scale setup. The absence of any significant differences in the photocatalytic activity of BiOBr11/LECA in the two different bowls indicates that the lateral illumination of the bowl has a minor effect compared to the importance of direct lighting from the top.

The entire setup was subjected to four other reuses to test the stability of the floating photocatalyst. At the end of each test, the composite was washed with deionized water and reused. **Figure 9** displays the activity of the studied floating photocatalyst in the DCF abatement. More in detail, DCF abatement higher than 60% was detected, except in the second reuse, when only ≈ 38% DCF abatement was observed after 10 h light irradiation due to the lower daily solar irradiation (only ≈ 51.9 $W \cdot m^{-2}$) than the other cases. In contrast, IBU was never completely abated, and the decrease in the capability of BiOBr11/LECA to remove it was detected over the successive reuses, probably ascribable to the gradual saturation of the active sites by traces of DCF's TPs.

3. Conclusion

In this study, floating photocatalysts consisting of BiOBr grown on a material derived from natural sources, specifically Lightweight Expanded Clay Aggregates (LECA), were successfully fabricated. They were designed to remove two commonly found non-steroidal anti-inflammatory drugs, ibuprofen, and diclofenac, under various environmental conditions. Real-scale tests on these photocatalysts demonstrated highly promising results in terms of diclofenac (DCF) degradation, whereas the degradation of ibuprofen (IBU) was limited and related to the DCF content in the solution. Through UPLC/MS investigations, we observed the presence of a specific transformation product

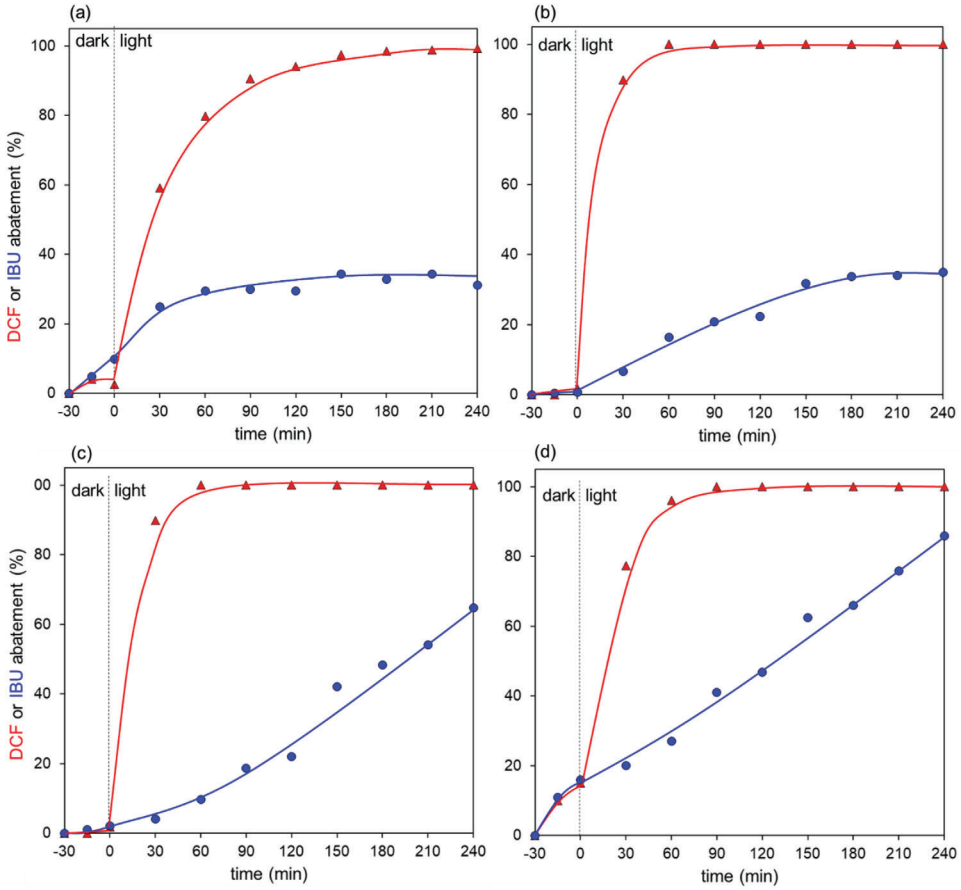

Figure 7. Photodegradation results of 50 mg·L^{-1} drugs mixture (DCF/IBU weight ratio: a) 6:1, b) 3:1, c) 1:3, and d) 1:6) in UW by 3 g BiOBr11/LECA. Solar light irradiation = 35 W·m^{-2}.

(TP) formed by the dechlorination of diclofenac during the photodegradation reaction. The fast formation of this TP justifies the rapid DCF disappearance and seems responsible for the restricted IBU degradation. Although the precise mechanism causing this inhibition is not yet fully understood, it appears to be linked to the adsorption of this TP onto the active sites of the catalysts, resulting in their deactivation. In conclusion, these findings suggest that BiOBr/LECA has the potential to serve as a promising sustainable alternative to traditional materials for the effective removal of pharmaceutical drugs from water.

4. Experimental Section

Chemicals and Materials: All reactants were of analytical grade and supplied by Sigma Aldrich. Ultrapure water was obtained by the Milli-Q ultra-pure water system from Merck Millipore. LECA was from Geolia, Brico (lot 1324 at controlled pH). Pyrex glass bowl (diameter of 19 cm, height of 9.5 cm) was purchased by Colaver s.r.l., whereas the plastic one, in white polypropylene (232 × 276 × 138 mm), comes from GP&meItaly.

Preparation of Bismuth Oxybromide Supported Onto Lightweight Expanded Clay Aggregate (BiOBr/LECA) Samples: Before any treatments, pristine LECA was washed with abundant deionized water and ethanol to remove any impurities, dried at 100 °C for 2 h, and successively maintained at room temperature overnight. BiOBr/LECA composites were prepared via wet impregnation according to the following method, taking inspiration from Wang et al.[58] In a typical preparation, ≈ 30 g pristine LECA was immersed first in 273 mL 0.1 M $Bi(NO_3)_3{\cdot}5H_2O$ aqueous solution containing 10 wt.% glacial acetic acid for 1 min and then in 200 mL 0.1 M KBr for 1 min. The resulting sample was dried at 120 °C for 15 min, and then a successive treatment was carried out. In each of the five subsequent treatments, both solutions were replaced with fresh ones. The described procedure was repeated several times up to reach 3, 6, and 11 wt.% BiOBr loading on LECA. The as-obtained samples were calcined at 200 °C for 2 h, washed several times with deionized water, sonicated to remove the excess of BiOBr not anchored on LECA, eventually washed several times with ultrapure water, and dried at 120 °C for 30 min. This procedure was necessary to ensure the homogeneous BiOBr growth onto the LECA surface without releasing BiOBr from LECA during the successive photodegradation tests. The resulting samples were labeled as BiOBrX/LECA, where X is the BiOBr loading in wt.%. The amount of BiOBr on LECA (in wt.%) was computed according to the following equation:

$$\text{wt.\%BiOBr} = \frac{\text{final weight}_{\text{BiOBronLECA}} - \text{starting weight}_{\text{BiOBronLECA}}}{\text{final weight}_{\text{BiOBronLECA}}} \times 100\% \quad (1)$$

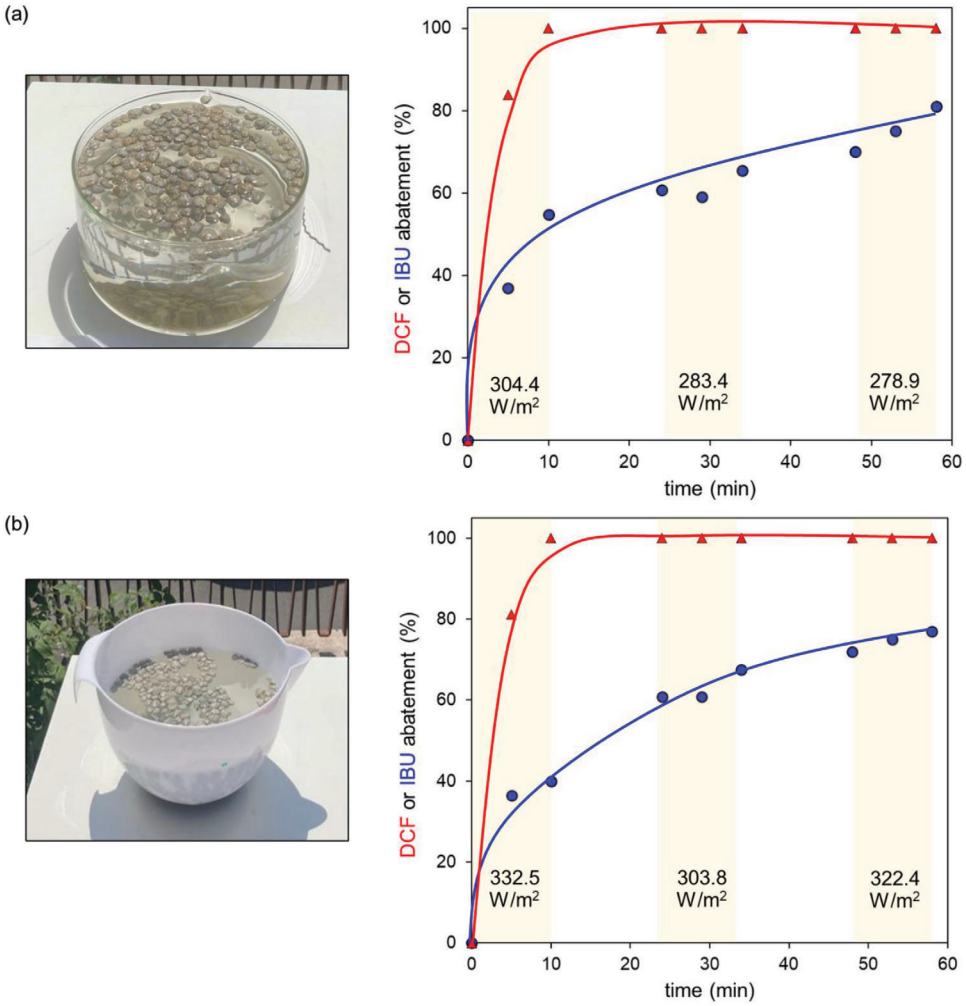

Figure 8. Real-scale results of photodegradation of an IBU and DCF mixture (3:1 weight ratio, total drugs concentration = 10 mg·L^{-1}) in the presence of 60 g BiOBr11/LECA in DW in the glass or plastic containers under natural solar light. Data of the daily medium solar irradiation (in W·m^{-2}) were detected by the meteorological station of Milano Lambrate, Italy.[57].

Characterization: Pore size distribution (PSD) of the pristine LECA was determined by applying Barrett-Joyner-Halenda (BJH) model to the desorption branch of N_2 adsorption/desorption isotherms collected at −196 °C in the 0.3-0.95 p/p^0 window. Before the analysis, the sample was pretreated at 150 °C for 4 h under vacuum.

Morphology and elemental analyses of pristine LECA and BiOBr11/LECA were obtained with the scanning electron microscope operating with a Field Emission source, model TESCAN S9000G (Over-coached, Germany) with a source of Schottky type FEG (resolution of 0.7 nm at 15 keV in In-Beam SE mode) equipped with EDS Oxford Ultim Max (operated with Az-tec software 6.0). Samples were supported on metallic stabs with C tape and then coated with Cr using the ion-sputtering technique to improve the materials' conductivity.

The crystal structure and phase composition of LECA and BiOBr11/LECA were determined by X-ray powder diffraction (XRPD) using a PANanalytical X'Pert PRO diffractometer (Cu Kα = 1.54060 Å, X-ray source at 40 kV × 40 mA). Before any analysis, samples were crushed to obtain fine ground powder and spread on an aluminum flat-plate horizontal sample holder. Diffractograms were collected in the 10–70° (2θ) range (2θ step of 0.02°, time per each step in 5–96 s intervals) and they were compared to the XRPD patterns of BiOBr and LECA reported in the JCPDS files (International Center for Diffraction Data Powder).

The point of zero charge (pH_{pzc}) of the pristine LECA and BiOBr11/LECA was determined following the previous works.[13] About 100 mg of each sample was contacted with 20 mL $NaNO_3$ 0.1 M solutions under stirring (250 rpm). The initial solution pH values ($pH_{initial}$) were by adding 0.1 M HNO_3 or NaOH to drop in 4.00–10.00 window. The as-obtained suspensions were maintained under stirring (250 rpm). They were centrifuged (3000 rpm for 10 min) after 24 h, and the final pH values (pH_{final}) were measured. By plotting the difference between the pH_{final} and $pH_{initial}$ (ΔpH) along with the $pH_{initial}$, pH_{pzc} was determined as the intersection of the resulting line at which $\Delta pH = 0$.

Photocatalytic Experiments: Ibuprofen (IBU), and diclofenac (DCF) were selected as model drugs: their adsorption and photo-

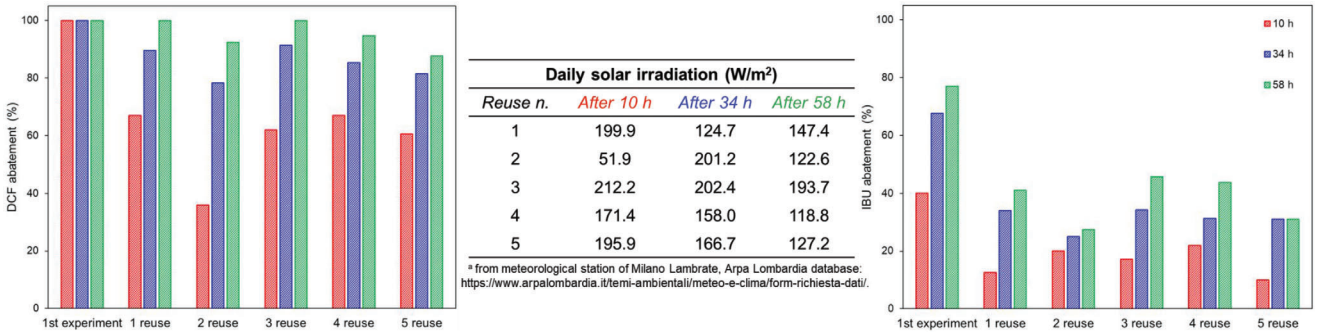

Daily solar irradiation (W/m^2)

Reuse n.	After 10 h	After 34 h	After 58 h
1	199.9	124.7	147.4
2	51.9	201.2	122.6
3	212.2	202.4	193.7
4	171.4	158.0	118.8
5	195.9	166.7	127.2

[a] from meteorological station of Milano Lambrate, Arpa Lombardia database: https://www.arpalombardia.it/temi-ambientali/meteo-e-clima/form-richiesta-dati/.

Figure 9. Real-scale reusability results of photodegradation of an IBU and DCF mixture (3:1 weight ratio, total drugs concentration = 10 $mg{\cdot}L^{-1}$) in DW by 60 g BiOBr11/LECA in a plastic container under natural solar light. Data from the first experiment comes from Figure 8. Data of the daily medium solar irradiation (in $W{\cdot}m^{-2}$) were detected by the meteorological station of Milano Lambrate, Italy.[57]

catalytic degradation were monitored in the dark and under solar light irradiation, as reported below.

Two different types of tests were performed: laboratory- and real-scale tests in ultrapure or simulated drinking water (UW and DW, respectively). DW was prepared according to Annex B2 of the second protocol of the French Norm NF P41-650.[59] Table S1 (Supporting Information) summarizes its main composition.

Laboratory-Scale Experiments: Experiments were performed under atmospheric conditions in 250 mL batch glass cylindric reactor inserted in a homemade box with dark walls made of cloth. A solar lamp (ULTRA VITALUX 300W-OSRAM, irradiation power density of 35 $W{\cdot}m^{-2}$) was installed above the reactor at fixed height (25 cm). The proper amount of pristine LECA or BiOBrX/LECA (≈ 3 g) and 100 mL solution of pollutant(s), single or in mixture (with different drug ratios), at different concentrations (10–50 $mg{\cdot}L^{-1}$) were stirred (250 rpm) in the dark for 30 min and then irradiated for 240 min. Tests were carried out at spontaneous pH depending on the type of water matrix used (≈ 7 in UW and 7.5 in DW). Each test was repeated three times to ensure reproducibility: in any case, a percent relative uncertainty <5 % was obtained.

Real-Scale Experiments: Two liters of 10 $mg{\cdot}L^{-1}$ solution of pollutant(s), single or in mixture (with different drug ratios), were put in a glass or plastic white bowl. Then, 30 g floating photocatalyst was introduced, and the mixture was exposed to the natural solar light from 9:00 am to 6:00 pm for three days (for a total of 27 h exposure to solar irradiation, i.e., 9 h per day). Data of the daily medium solar irradiation (in $W{\cdot}m^{-2}$) were detected by the meteorological station of Milano Lambrate, Italy.[57] The bowl was covered during the night (15 h per each) to avoid water evaporation. Moreover, the adsorption properties were investigated in the dark for both vessels (glass and plastic bowls) (Figure S7, Supporting Information).

Monitoring of Drug Abatement: IBU and DCF abatement was monitored for a total of 240 min and 3 days in lab- and real-scale tests, respectively. In laboratory-scale tests, 2 mL aliquots were sampled every 15 min for the dark region and every 30 min for the irradiated region, whereas in the real ones, 2 mL aliquots were taken every 4 h during the exposition to the natural solar light. The collected aliquots were placed in 1.5 mL conical vials and centrifuged with a LaboGene ScanSpeed centrifuge at 13 500 rpm for 10 min before any analyses. They were then quantitatively analyzed by an HPLC/UV instrument (Agilent 1100 Series) equipped with a C18 Supelco column (25 cm × 4 mm, 5 µm), a 20 µL injection loop, and a UV detector. Chromatographic analyses were performed with an isocratic elution of a mobile phase composed of 50% water, 50% acetonitrile, and 0.1% formic acid at 1 $mL{\cdot}min^{-1}$ flow rate. The IBU and DCF disappearance was monitored at 230 and 276 nm, respectively, whereas the formation of by-products was followed at 260 nm. Drugs abatement (%) was calculated according to the following equation:

$$\text{Drug abatement}(\%) = \frac{C_0 - C_t}{C_0} \times 100\% \quad (2)$$

where C_0 is the initial drug concentration, and C_t is the drug concentration at the time t.

Because LECA causes a slight release of organic material in solution that compromises the results of TOC (Total Organic Carbon) analyses, the mineralization capacity of the floating composites was not evaluated. In contrast, the mineralization ability of BiOBr powder was properly verified.

Transformation products (TPs) were recognized by UPLC/MS analyses carried out on a ThermoFisher (Waltham, MA, USA) LCQ Fleet ion trap mass spectrometer equipped with an HPLC UltiMate 3000 system containing UV detector. A Zorbax RX-C18 (2.1 × 150 mm, 5 µm) column was maintained at 30 °C. The same chromatographic conditions used for the HPLC/UV were employed. The mass spectrometer operated with electrospray ionization in positive and negative ion modes. Full-scan mass spectra were recorded in the 50–900 mass/charge (m/z) range.

Supporting Information

Supporting Information is available from the Wiley Online Library or from the author.

Acknowledgements

Velux Stiftung Foundation was gratefully acknowledged for their financial support through project 1381 "SUNFLOAT—Water decontamination by sunlight-driven floating photocatalytic systems".

Conflict of Interest

The authors declare no conflict of interest.

Data Availability Statement

The data that support the findings of this study are available from the corresponding author upon reasonable request.

Keywords

diclofenac, eco-friendly material, ibuprofen, non-steroidal anti-inflammatory drugs, surface water treatment, sustainable floating photocatalysts

Received: November 16, 2023
Revised: January 24, 2024
Published online: February 7, 2024

[1] Water scarcity, https://www.fao.org/land-water/water/water-scarcity/en/, accessed: October, **2023**.
[2] *Centers for Disease Control and Prevention*, https://www.cdc.gov/healthywater/drinking/public/water_diseases, accessed: October **2023**.
[3] World Health Organization, https://www.who.int/news/item/14-12-2020-almost-2-billion-people-depend-on-health-care-facilities-without-basic-water-services-who-unicef, accessed: October **2023**.
[4] S. Chopra, D. Kumar, *Heliyon* **2020**, *6*, e04087.
[5] *Fortune Business Insights*, https://www.fortunebusinessinsights.com/non-steroidal-anti-inflammatory-drugs-nsaids-market-102823, accessed: September **2023**.
[6] I. Georgaki, E. Vasilaki, N. Katsaralis, *Am. J. An. Chem.* **2014**, *5*, 519.
[7] H. Gong, W. Chu, Y. Huang, L. Xu, M. Chen, M. Yan, *Env. Poll.* **2021**, *276*, 116691.
[8] C. Yuan, C. H. Hung, H. W. Li, W. H. Chang, *Chemosphere* **2016**, *155*, 471.
[9] N. Miranda-Garcia, S. Suarez, B. Sanchez, J. M. Coronado, S. Malato, M. I. Maldonado, *Appl. Catal. B* **2011**, *103*, 294.
[10] N. Klamerth, L. Rizzo, S. Malato, M. I. Maldonado, A. Aguera, A. R. Fernandez-Alba, *Water Res.* **2010**, *44*, 545.
[11] D. Grace, J. Rogers, K. Skeith, K. Anderson, *J. Rheumatol.* **1999**, *12*, 2659.
[12] P. John, K. Johari, N. Gnanasundaram, A. Appusamy, M. Thanabalan, *Env. Technol. Innov.* **2021**, *22*, 101412.
[13] M. G. Galloni, G. Cerrato, A. Giordana, E. Falletta, C. L. Bianchi, *Catalysts* **2022**, *12*, 804.
[14] D. Meroni, C. L. Bianchi, D. C. Boffito, G. Cerrato, A. Bruni, M. Sartirana, E. Falletta, *Ultrason. Sonochem.* **2021**, *75*, 105615.
[15] A. Michalaki, K. Grintzalis, *Toxics* **2023**, *11*, 320.
[16] S. Murgolo, S. Franz, H. Arab, M. Bestetti, E. Falletta, *Water Res.* **2019**, *164*, 114920.
[17] R. Djellabi, R. Giannantonio, E. Falletta, C. L. Bianchi, *Curr. Op. in Chem. Eng.* **2021**, *33*, 100696.
[18] D. Meroni, M. G. Galloni, C. Cionti, G. Cerrato, E. Falletta, C. L. Bianchi, *Materials* **2023**, *16*, 1304.
[19] R. Djellabi, D. Aboagye, M. G. Galloni, V. V. Andhalkar, S. Nouacer, W. Nabgan, S. Rtimi, M. Constanti, F. Medina Cabello, S. Contreras, *Bioresour. Technol.* **2023**, *368*, 128333.
[20] M. G. Galloni, E. Ferrara, E. Falletta, C. L. Bianchi, *Catalysts* **2022**, *12*, 923.
[21] D. Ma, H. Yi, C. Lai, X. Liu, X. Huo, Z. An, L. Li, Y. Fu, B. Li, M. Zhang, L. Qin, S. Liu, L. Yang, *Chemosphere* **2021**, *275*, 130104.
[22] A. L. Linsebigler, G. Lu, J. T. Yates, *Chem. Rev.* **1995**, *95*, 735.
[23] X. Chen, L. Qiao, R. Zhao, J. Wu, J. Gao, L. Li, J. Chen, W. Wang, M. G. Galloni, F. M. Scesa, Z. Chen, E. Falletta, *J. Env. Chem. Eng.* **2023**, *11*, 109416.
[24] J. A. Rengifo-Herrera, C. Pulgarin, *Chem. Eng. J.* **2023**, *477*, 146875.
[25] A. S. Sa, R. P. Feitosa, L. Honorio, R. Pena-Garcia, L. C. Almeida, J. S. Dias, L. P. Brazuna, T. G. Tabuti, E. R. Triboni, J. A. Osajima, E. C. da Silva-Filho, *Materials* **2021**, *14*, 5891.
[26] L. C. Manikanika, *Mater. Tod.: Proceed.* **2022**, *52*, 1653.
[27] M. E. Malefane, U. Feleni, P. J. Mafa, A. T. Kuvarega, *Appl. Surf. Sci.* **2020**, *514*, 145940.
[28] A. Kezzim, A. Boudjemaa, A. Belhadi, M. Trari, *Res. Chem. Intermed.* **2016**, *43*, 3727.
[29] M. Ma, Y. Yang, Y. Chen, J. Jiang, Y. Ma, Z. Wang, W. Huang, S. Wang, M. Liu, D. Ma, X. Yan, *Sci. Rep.* **2021**, *11*, 2597.
[30] M. Ma, Y. Yang, Y. Chen, Y. Ma, P. Lyu, A. Cui, W. Huang, Z. Zhang, Y. Li, F. Si, *J. Alloys Compd.* **2021**, *861*, 158256.
[31] Z. Xing, J. Zhang, J. Cui, J. Yin, T. Zhao, J. Kuang, Z. Xiu, N. Wan, W. Zhou, *Appl. Catal. B* **2018**, *225*, 452.
[32] Z. Xing, Z. Xing, H. Zhang, Z. Li, X. Zhang, Y. Zhang, L. Li, W. Zhou, *ChemPlusChem* **2015**, *80*, 623.
[33] L. P. D'Souza, S. Shree, G. R. Balakrishna, *Ind. Eng. Chem. Res.* **2013**, *52*, 16162.
[34] M. Sutisna, E. Rokhmat, R. Wibowo, M. Murniati, K. Abdullah, *Adv. Mater. Res.* **2015**, *1112*, 149.
[35] M. G. Galloni, V. Bortolotto, E. Falletta, C. L. Bianchi, *Polymers* **2022**, *14*, 4897.
[36] M. L. Matias, M. Morais, A. Pimentel, F. X. Vasconcelos, A. S. Reis Machado, J. Rodrigues, E. Fortunato, R. Martins, D. Nunes, *Sustainability* **2022**, *14*, 9645.
[37] E. Falletta, M. Longhi, A. Di Michele, D. C. Boffito, C. L. Bianchi, *J. Cleaner Prod.* **2022**, *371*, 133641.
[38] A. M. Nasir, J. Jaafar, F. Aziz, N. Yusof, W. N. Wan Salleh, A. F. Ismail, M. Aziz, *J. Water Proc. Eng.* **2020**, *36*, 101300.
[39] X. Fu, G. Zhou, J. Li, Q. Yao, Z. Han, R. Yang, X. Chen, Y. Wang, *Chemosphere* **2023**, *341*, 140043.
[40] R. Djellabi, L. Zhang, B. Yang, M. Rizwan Haider, X. Zhao, *Sep. Purif. Technol.* **2019**, *229*, 115830.
[41] A. M. Rashad, *Constr. Build. Mater.* **2018**, *170*, 757.
[42] R. Mlih, F. Bydalek, E. Klumpp, N. Yaghi, R. Bol, J. Wenk, *Ecol. Eng.* **2020**, *148*, 105783.
[43] E. M. Kalhori, K. Yetilmezsoy, N. Uygur, M. Zarrabi, R. M. Abu Shmeis, *Appl. Surf. Sci.* **2013**, *287*, 428.
[44] M. N. Sepehr, H. Kazemian, E. Ghahramani, A. Amrane, V. Sivasankar, M. Zarrabi, *Inst.Chem. Eng.* **2014**, *45*, 1821.
[45] E. M. Kalhori, T. J. Al-Musawi, E. Ghahramani, H. Kazemian, M. Zarrabi, *Chemosphere* **2017**, *175*, 8.
[46] M. Zendehzaban, S. Sharifnia, S. N. Hosseini, *Korean J. Chem. Eng.* **2013**, *30*, 574.
[47] Y. Shavisi, S. Sharifnia, M. Zendehzaban, M. Lobabi Mirghavami, S. Kakehazar, *J. Industr. Engin. Chem.* **2014**, *20*, 2806.
[48] Z. Mohammadi, S. Sharifnia, Y. Shavisi, *Mater. Chem. Phys.* **2016**, *184*, 110.
[49] H. Moradi, S. Sharifnia, F. Rahimpour, *Mater. Chem. Phys.* **2015**, *158*, 38.
[50] I. Ahmad, S. Shukrullah, M. Yasin Naz, S. Ullah, M. Ali Assiri, *J. Industr. Engin. Chem.* **2022**, *105*, 1.
[51] X. Lv, F. L. Yuk Lam, X. Hu, *Front. Catal.* **2022**, *2*, 1.
[52] J. Liu, H. Deng, *J. Env. Chem. Eng.* **2023**, *11*, 110311.
[53] E. Falletta, M. G. Galloni, N. Mila, M. N. bin Roslan, N. A. Ghani, G. Cerrato, A. Giordana, M. Magni, S. Spriano, D. C. Boffito, C. L. Bianchi, *ACS Photonics* **2023**, *10*, 3929.
[54] E. N. Bakatula, D. Richard, C. M. Neculita, *Environ. Sci. Pollut. Res.* **2018**, *25*, 7823.
[55] R. H. Yoon, T. Salman, G. Donnay, *J. Colloids Interface Sci.* **1979**, *70*, 483.

[56] *PubChem*, https://pubchem.ncbi.nlm.nih.gov, accessed: September, **2023**.
[57] *Arpa Lombardia*, https://www.arpalombardia.it/temi-ambientali/meteo-e-clima/form-richiesta-dati/, accessed: July, **2023**.
[58] W. Wang, Y. Zhang, T. Zhang, F. Dong, H. Huang, *Appl. Catal. B* **2017**, *208*, 75.
[59] L. Rimoldi, D. Meroni, E. Falletta, V. Pifferi, L. Falciola, G. Cappelletti, S. Ardizzone, *Photochem. Photobiol. Sci.* **2017**, *16*, 60.